PCCP

Cite this: *Phys. Chem. Chem. Phys.*, 2011, **13**, 10131–10135

www.rsc.org/pccp

PAPER

Tunable catalytic tubular micro-pumps operating at low concentrations of hydrogen peroxide†

Alexander A. Solovev,* Samuel Sanchez,* Yongfeng Mei‡ and Oliver G. Schmidt

Received 28th February 2011, Accepted 1st April 2011
DOI: 10.1039/c1cp20542k

Catalytic micropumps consisting of Ti/Cr/Pt microtubes with diameters of 5–10 μm and tunable lengths in the range of 20–1000 μm are reported. Micropumps were fabricated by rolling up metallic nanomembranes into microtubes with an inner platinum layer. When immersed into a solution of hydrogen peroxide, the micropumps are activated by the catalytic decomposition of peroxide into oxygen microbubbles and water. Fluid pumping is demonstrated by the movement of polystyrene particles with a diameter of 1 μm through the catalytic microtubes. Concentrations from 0.009 to 11% H_2O_2 were employed to study the catalytic generation of microbubbles in micropumps with different lengths. A minimum concentration of 0.06% fuel was determined to be sufficient to actuate the micropumps. Such devices based on rolled-up nanomembranes hold great promise for the integration into Lab-on-a-chip systems for sensing, sorting of particles and drug delivery.

Introduction

Nowadays, pumping, mixing and moving fluids on the small scale are essential for miniaturization of conventional research tools into microfluidics.[1] Microscale pumps have numerous applications and are widely used in ink-jet printing,[2] drug delivery and biochemical sensing,[3] fluid transportation on a single chip[4] and even in remotely powered self-propelled devices.[5]

Fluid pumping at the microscale is challenging due to the high viscosity of fluids dominating at low Reynolds numbers.[6] It has been demonstrated previously that it is possible to induce fluid motion by external sources based on electrical,[7] electrochemical[8] and thermal[9] principles, for instance. An elegant way of pumping fluid without external pumps or sources relies on the catalytic reactions that can take place on the surfaces of the microfluidic pumps. In particular, electrokinetic pumping based on the decomposition of hydrogen peroxide into oxygen and water was recently realized on planar catalytic bimetallic surfaces.[10,11] In comparison to previously reported catalytic pumping on planar substrate surfaces, tubular catalytic micropumps offer compact fluid pumping as well as easy integration into Lab-on-a-Chip devices and self-propelled micromachines. Previously, Schmidt and Eberl have suggested to generate tiny bubbles in fluids ejected from rolled-up micro-/nanotubes[12] and these bubbles have later been exploited to self-propel catalytic jet engines.[13–18] The catalytic decomposition of hydrogen peroxide in contact with the platinum contained in the inside of the microtubes has been well described previously.[15,19]

Here we report on the fabrication of arrays of tubular micropumps on a chip, relying on tube fabrication on polymers.[13,19] In the present approach, microtubes are fixed on the substrate and by making use of the catalytic reaction inside, the pumping of fluid through the hollow structure is achieved. We demonstrate the directed motion of polystyrene microparticles through the microtubular pumps, and we study the optimum concentration range suitable for unidirectional fluid motion. A minimum peroxide concentration of 0.06% v/v was found to be sufficient to generate microbubbles, which is two orders of magnitude lower than reported previously for larger micropumps.[20] Furthermore, the integration of non-catalytic rolled-up microtubes into microfluidic devices was previously demonstrated[21] by our group. Thus, we believe that our findings in self-actuated micropumps will be beneficial for self-pumping of fluids and directed transport and sorting of objects without the need of external sources.

Experimental

Fabrication of rolled-up microtubes

The fabrication of rolled-up microtubes consisting of Ti/Cr/Pt nanomembranes (10/10/1 nm) was performed as follows. Photoresist AR-P 3510 was spin-coated on silicon wafers

Institute for Integrative Nanosciences, IFW Dresden, Helmholzstr 20, D-01069 Dresden, Germany. E-mail: a.solovev@ifw-dresden.de, s.sanchez@ifw-dresden.de; Fax: +49 (0)351 4659 782; Tel: +49 (0)351 4659 845

† Electronic supplementary information (ESI) available: All supplementary videos are real time. (1) Video 1 for Fig. 1. (2) Video 2 for Fig. 1. (3) Video 3 for Fig. 2. (4) Video 4 for Fig. 2. (5) Video 5 for Fig. 3. (6) Video 6 for Fig. 3. (7) Video 7 for Fig. 5. See DOI: 10.1039/c1cp20542k

‡ Current address: Department of Materials Science, Fudan University, Shanghai, 200433, Peoples's Republic of China.

(1.5 inch) at 3500 rpm for 35 s, followed by a soft bake using a hot plate at 90 °C for 1 min and 7 s exposure to UV light with a Karl Suss MA-56 Mask Aligner (410–605 nm). Photoresist patterns were then developed in an AR300-35 : H_2O solution (1 : 1). The Ti/Cr thin membranes were deposited by electron-beam (e-beam) evaporation, whereas the Pt layers were deposited by magnetron sputtering.

Ti/Cr layers of 10/10 nm were prepared by Edwards Thin Film Systems at evaporation rates of 2.0 and 1.5 Å s^{-1}, respectively, with an initial chamber pressure of 5×10^{-7} mbar. Pt was sputtered by using MTD 450 DCA instruments machine with a total thickness of 1 nm at 4.4 nm min^{-1}. Samples deposited by e-beam were tilted to an angle of 75°. However, we performed a flat sputtering (0°) for the Pt deposition. After deposition of the metals, the samples were immersed in acetone that selectively underetches the photoresist layer and consequently the rolling-up of the thin metallic films into microtubes takes place. Supercritical point drying was used in order to avoid tubes collapsing due to the high fluid surface tension.

Rolled-up microtubes as catalytic micropumps

In order to activate the micropumps, we soaked the fabricated arrays of microtubes with hydrogen peroxide solutions containing benzalkonium chloride (BC) at 0.5 v/v% which is needed to reduce the surface tension at the inner tube–solution interface and stabilize the released oxygen microbubbles. The surfactant concentration was optimized and kept constant along the experiments reported in this work. The concentration of the hydrogen peroxide was varied from 0.009 to 11 v/v%. Catalytic micropumps were analyzed by a high speed camera (Photonic Science Limited) generating 50–200 frames per second, coupled to a Zeiss Axio Microscope. Videos were analyzed using VirtualDub and ImageJ software.

Polystyrene microspheres (Duke Scientific Corp., 1% Solids) with diameters of 1 μm and 7 μm were used in the experiments for particle pumping.

Results and discussion

The directed and autonomous fluid pumping and the controlled manipulation of microobjects in solution are important for miniaturized systems[22,23] and chemically powered micro- and nanomachines.[13–19,24] For reaching that purpose, we design arrays of microtubular structures containing catalytic surfaces in their interior. As a representative example, Fig. 1A (left) shows an optical microscopy image of a 100 μm long Ti/Cr/Pt micropump immersed in an aqueous solution of hydrogen peroxide (1.0% v/v H_2O_2, 0.5% v/v BC). The platinum surface at the inside of the micropump inititates the catalytic decomposition of dilute H_2O_2 solutions inducing the motion of fluid. The direction of the fluid is governed, in principle, by the slight asymmetry of the tube geometry, causing the fluid to move towards the larger opening which is visualized in Fig. 1A by the transport of polystyrene microparticles. As a result, particles with a diameter smaller than the microtube, *i.e.* $d_p < d_t$, are sucked into the micropump, Fig. 1A. A slow oscillation of the microparticles near the pump mouth is attributed to the growth and recoil of microbubbles within the micropump,

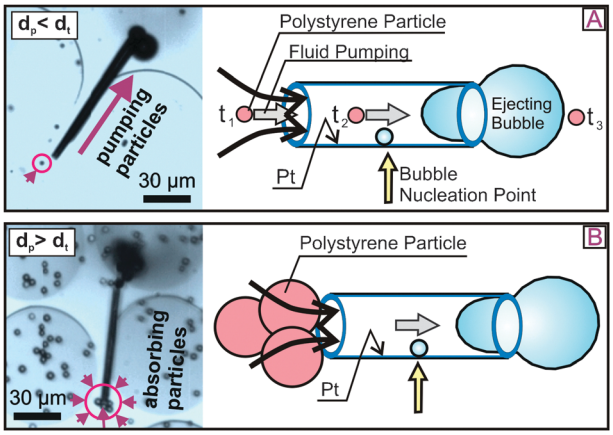

Fig. 1 Catalytic pumping of polystyrene particles by Ti/Cr/Pt microtubes. (A) Left: optical microscopy image showing a rolled up micropump on a silicon substrate sucking in a small microparticle. Right: sketch showing the nucleation and release of microbubbles out of the micropump. (B) Left: optical microscopy image showing large microparticles absorbed at the mouth of the micropump. Right: sketch of the process taking place. Grey arrows indicate the direction of the fluid flow.

clearly observed in S-Video 1 (ESI†). At time t_1, the particle follows the fluid streamlines, then comes into the micropump body (t_2) and finally is pumped out (t_3). Therefore, the motion of the particles is synchronized with the growth and migration of microbubbles which displaces fluids within the micropump. Fig. 1B (left) shows an optical microscopy image of the polystyrene microparticles with 7 μm diameter, which are larger than the mouth of the micropump, $d_p > d_t$. In this scenario, particles are absorbed at the entrance of the micropump (S-Video 2, ESI†) while the micropump is still active. Fig. 1B (right) shows a schematic diagram of the absorbed particles at the micropump mouth. These large microparticles do not block completely the entrance of the tube as can be confirmed by the continuous generation of microbubbles coming out from the opposite opening. A similar phenomenon was observed previously in catalytic microjet engines transporting large microparticles[15,17] and cells.[18] The presented results are a proof that catalytic microtubes, while decomposing H_2O_2, induce the motion and thus the pumping of fluid inside their hollow structure. Furthermore, the micropumps are capable of moving particles into and through their body. Since the diameter of the microtubes can be tailored, the tubular micropumps could be used for sorting of particles with different sizes.

A more detailed study regarding the pumping of particles is shown in Fig. 2 where a microparticle can be visualized and tracked through the micropump. For this purpose, we select a micropump with length 40 μm and diameter 5.6 μm, *i.e.* with an aspect ratio of 7. Fig. 2A–D shows the pumping of an individual polystyrene microparticle with a diameter of 1 μm accomplished over 580 ms. This micropump operates at an average frequency of 7 bubbles per second (fuel: 1.0% v/v H_2O_2, 0.5% v/v BC, see S-Video 3, ESI†) measured over 15 seconds. At the time $t = 0$ ms, the particle is located in close proximity to the mouth of the micropump. When a bubble inside the micropump migrates and finally recoils at $t = 135$ ms,

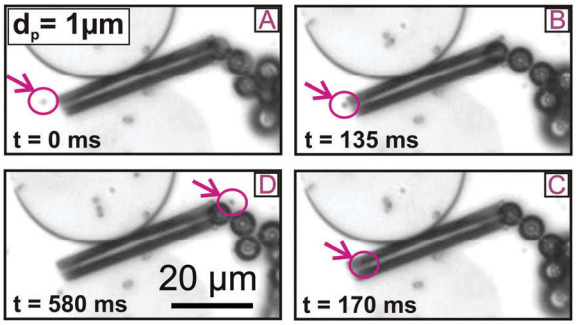

Fig. 2 Sequence of optical images of a tubular micropump which moves microparticles through its hollow body. Arrows show a tracked individual polystyrene microparticle with a diameter of 1 μm. At the time t = 0 ms (A), the particle comes into close proximity of the micropump mouth, at 135 ms approaches entrance (B), at t = 170 ms is sucked inside (C) and after 580 ms is pumped out (D). Large black spheres exiting the micropump are oxygen microbubbles.

the tracked microparticle moves immediately closer to the mouth. Afterwards, the motion of the next microbubble through the tube sucks more fuel bringing along the particle into the micropump where it remains until t = 580 ms when it is released together with the next microbubble. S-Video 4 (ESI†) shows another micropump with the same length operating at an average frequency of 40 bubbles per second (fuel: 4.0% v/v H_2O_2, 0.5% v/v BC). Therefore, an increase of the peroxide concentration leads to a higher pumping activity, similar to what has been reported before for catalytic microjet engines.[14,15] We previously hypothesized that mainly a change of the microtube diameter (conical shape) leads to an asymmetric release of bubbles only from the larger tubular opening.[14,15] However, a clear conical shape is not always detectable by optical microscopy, as shown in Fig. 2, and additionally a generation of bubbles in both directions has been observed.

It is of particular interest to pump fluid in unidirectional fashion.[25] Indeed, for practical applications, the fluidic micropump remains a useful device only if it is not 'overloaded', *i.e.* when bubbles recoil and a fluid is pumped only in one direction. Hence, it is important to investigate and control the conditions in which the microtubes can generate microbubbles at one or both ends. Fig. 3 illustrates the change in directionality of the pumping depending on the concentration of H_2O_2 for 100 μm long Ti/Cr/Pt micropumps. Fig. 3A and B shows optical microscopy images (bottom) and schematics (top) of the 'unidirectional' (Fig. 3A and S-Video 5, ESI†) and the 'overloaded' (Fig. 3B and S-Video 6) pumping regimes.

To obtain statistical data we have tested 20 different micropumps per silicon substrate. The data showed reproducible results for different samples. It is found that at a concentration of the peroxide fuel below 3 v/v% H_2O_2, Fig. 3C left y-axis, not all catalytic micropumps are activated. However, by increasing the fuel concentration up to 3 v/v%, we achieve activation of all micropumps. Interestingly, when the concentration of peroxide is above 0.5% v/v, the unidirectionality of the bubbles recoil is broken, Fig. 3C right y-axis. The number of micropumps which remain pumping in one direction decreases dramatically from 100% at 0.5% H_2O_2 to 40% at 1% H_2O_2. However, when all the tubes are

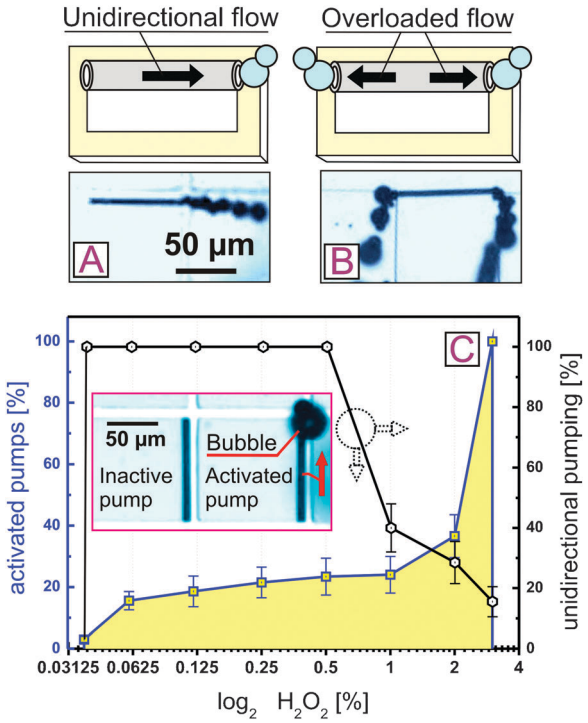

Fig. 3 Characterization of the microbubbles recoil for the pumps with a length of 100 μm. Optical microscopy image and schematic diagram of (A) the unidirectional and (B) the overloaded fluid flow. (C) Percentage of activated micropumps and unidirectional flow regime with different concentrations of the hydrogen peroxide. The inset shows inactive and activated micropumps. Red arrow indicates the direction of flow within the tubes.

active (*i.e.* at 3% H_2O_2), only 15.5% of them are pumping unidirectionally. At 1 v/v% of H_2O_2 approximately 60% of the micropumps experienced overloading, however not all of them were activated (76% remained inactive).

To explain this phenomenon, we hypothesize that in the region above 0.5 v/v% peroxide, the catalytic generation of microbubbles is so large that there is a limitation of physical space inside the tubular micropump. At lower concentrations, a steady-state of directional flow is created when bubbles moving within the tube draw new peroxide from one end (see scheme in Fig. 1A). Since the migration of bubbles within the tube is slower than the generation of new bubbles, they may collide inside the micropump causing the bubbles to eventually move towards the opposite direction thus exiting from both tubular openings. Similarly, the accumulation of bubbles in a microtube at high peroxide concentration was also observed for catalytic microbots, which was transferred to a saturation *plateau* of their speed upon an increase of the peroxide concentration.[15]

We studied the effect of hydrogen peroxide concentration on the bubble frequency and size for 100 μm long micropumps (Fig. 4). The bubble frequency increases upon increasing the fuel concentration, *i.e.* from 2 to 25.8 Hz. Thus, at higher peroxide concentrations, the required time for bubble nucleation and release is shorter than at lower concentrations. We observed that the bubbles which remain connected to the tube for longer times can acquire larger radii. For example, at 4%

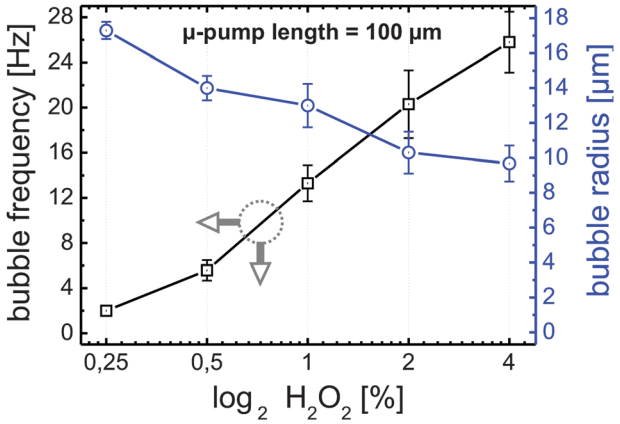

Fig. 4 Bubble frequency and radius with different hydrogen peroxide concentrations for micropumps of 100 μm in length.

H_2O_2 they are ejected after 0.052 s while at 0.5% H_2O_2 the bubbles are released every 0.35 s. As a consequence, the bubble radius diminishes from 17.3 μm to 9.7 μm correspondingly. Similar behaviour was previously observed in the bubble recoil from catalytic microjet engines.[14]

Because of the versatility of our fabrication technique, we can tailor the micropump sizes easily from 20 to 1000 μm length (Fig. 5). The length tunability allows for a full identification of the effective pumping working area (micropumps activity without overload) for each determined size. The region (i) in Fig. 5 represents inactive pumps where no microbubbles are observed, (ii) indicates an area where micropumps are active with unidirectional pumping, and (iii) shows the overloaded area (here at least one pump generated bubbles from two openings). Micropumps of 1000 μm length (S-Video 7, ESI†) require the lowest concentration of hydrogen peroxide to be active (0.009 v/v% H_2O_2) which is 750 times lower than the 20 μm long micropumps.

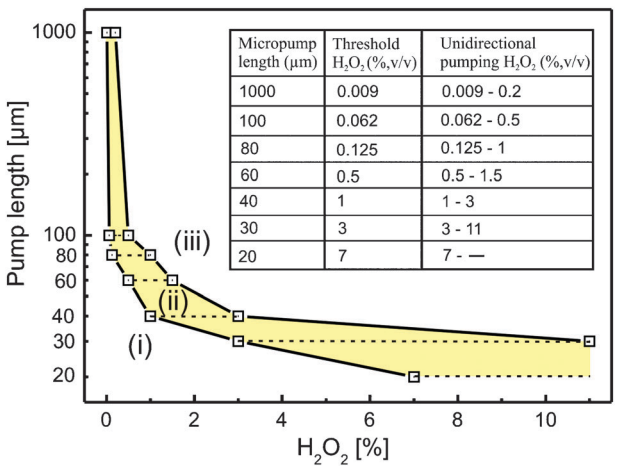

Micropump length (μm)	Threshold H_2O_2 (%,v/v)	Unidirectional pumping H_2O_2 (%,v/v)
1000	0.009	0.009 - 0.2
100	0.062	0.062 - 0.5
80	0.125	0.125 - 1
60	0.5	0.5 - 1.5
40	1	1 - 3
30	3	3 - 11
20	7	7 - —

Fig. 5 Activity regimes for variable Ti/Cr/Pt micropump lengths ranging from 20 to 1000 μm as a function of hydrogen peroxide concentration. Yellow region represents the working area for the unidirectional microbubbles recoil. Inset table shows details of data points shown in the graph, indicating a threshold peroxide concentration and unidirectional pumping range. Dashed horizontal lines show ranges of the peroxide concentrations suitable for unidirectional pumping.

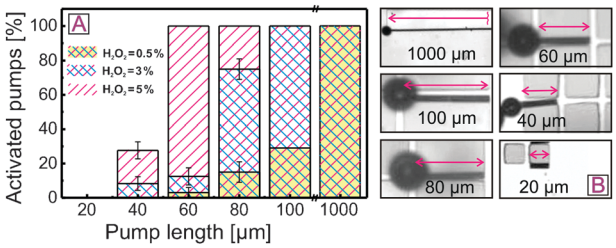

Fig. 6 (A) Population of activated micropumps in different concentrations of the hydrogen peroxide fuel. (B) Optical images of the catalytic micropumps with different lengths. Black rounds are microbubbles and arrow bars show lengths of the micropumps.

However, their range of unidirectional pumping remains only up to 0.2 v/v% H_2O_2 limiting their applicability. Micropumps of 100 μm length require peroxide fuel (0.062% H_2O_2) 16 times lower than for 20 μm micropumps, but their unidirectional pumping can be only extended up to 0.5% H_2O_2. A full working region of unidirectional pumping is shown in the inset table of Fig. 5. Each point represents an average measurement from 20 to 50 different micropumps. It is clearly observed in Fig. 5 that shorter tubes, *e.g.* 20–40 μm long, maintain their directional fluid motion (unidirectional pumping) for larger concentration ranges than longer tubes with, *e.g.* 60–1000 μm length. We studied 260 micropumps located in 2 different samples.

Fig. 6A depicts the population of activated micropumps with lengths ranging from 20 to 1000 μm soaked in three different concentrations of hydrogen peroxide of 0.5, 3 and 5 v/v%. At 0.5 v/v% H_2O_2, only 3% of the 60 μm long pumps, 15% of the 80 μm long pumps, 29.1% of the 100 μm long pumps and 100% of the 1 mm long pumps are activated. While increasing the H_2O_2 concentration up to 3 v/v%, 8.3% of the 40 μm pumps start to generate fluid motion by the generation of bubbles, 12.5% of 60 μm long pumps, and 75% of the 80 μm long pumps are active. Thus, shorter tubes need higher concentration of peroxide to be catalytically active. Finally, at 5 v/v% H_2O_2 all population of micropumps from 60–1000 μm long but only 27.7% of 40 μm pumps are active.

As discussed earlier (see also Fig. 5), 20 μm long micropumps require substantially higher concentration of the hydrogen peroxide fuel for catalytic generation of microbubbles. However, they are not overloaded even at higher peroxide concentrations which is in agreement with our previous hypothesis regarding the limitation of physical space for microbubbles within the microtube.

Fig. 5 and 6 reveal that the length of the microtube contributes significantly to the catalytic generation of oxygen microbubbles and consequently to the fluid motion inside the micropumps. Longer micropumps contain inherently a larger Pt catalyst surface area than shorter ones. For example, micropumps with length 1000 μm contain up to 125 times larger inner surface area of the catalyst than the 20 μm micropumps.

Therefore, the inactivity of short micropumps, Fig. 6A and B, at substantially high concentrations of the hydrogen peroxide shows that the rate of oxygen formation is limited by the surface area of the micropump. Furthermore, it has been shown before that microbubbles nucleate better if the catalytic surface contains

defects or cavities which reduce significantly the bubble nucleation energy barrier.[26] It is thus expected that longer tubes with larger catalytic surface area may contain more defects than shorter microtubes. These findings are of significant interest for current research on low toxicity fuels for self-propelled micromachines and integrated Lab-on-a-chip micropumps without the need of external driving sources.

Conclusions

In conclusion, we demostrated the fabrication of catalytic micropumps by rolling up nanomembranes into microtubes. Such micropumps have the advantages of being fully autonomous and requiring only very low concentration of chemical fuel (hydrogen peroxide) to be activated by the generation of oxygen microbubbles. It was shown that longer micropumps need less concentration of hydrogen peroxide to start pumping fluid in comparison to shorter micropumps. However, longer micropumps cannot provide unidirectional bubble recoil over a wide range of hydrogen peroxide fuels. The unidirectional flow has been used to move microparticles through the tubular structure in a directed way. The understanding of key aspects such as the catalyst turnover rate, catalyst surface area, concentration of the fuel, and existence of surface defects will permit the construction of more efficient pumping microdevices and micromachines. The use of reduced amounts of toxic fuels to efficiently move fluids by microengines is of current interest for future biomedical and sensing Lab-on-a-Chip applications. Such versatile micropumps may offer many advantages for not-too-distant integration into lab-in-a-tube analytical systems.[27]

Acknowledgements

The authors thank Cornelia Krien and Ronny Engelhardt for helping with preparation of samples and Dominic Thurmer for suggestions. A.A.S thanks Dr Guojiang Wang for fruitful discussion. This work was funded by the Volkswagen Foundation (I/84 072).

Notes and references

1 G. M. Whitesides, *Nature*, 2006, **442**, 368.
2 J. F. Dijksman, *Flow, Turbulence and Combustion*, Kluwer Academic Publishers, 1999, vol. 61, p. 211.
3 A. Nisar, N. Afzulpurkar, B. Mahaisavariya and A. Tuantranont, *Sens. Actuators, B*, 2008, **130**(2), 917; D. J. Laser and J. G. Santiago, *J. Micromech. Microeng.*, 2004, **14**, 35; P. Woias, *Sens. Actuators, B*, 2005, **105**, 28.
4 S.-H. Chiu and C.-H. Liu, *Lab Chip*, 2009, **9**, 1524.
5 S. T. Chang, V. N. Paunov, D. N. Petsev and O. D. Velev, *Nat. Mater.*, 2007, **6**, 235; S. T. Chang, E. Beaumont, D. N. Petsev and O. D. Velev, *Lab Chip*, 2008, **8**, 117.
6 E. M. Purcell, *Am. J. Phys.*, 1977, **45**, 3.
7 M. W. J. Prins, W. J. J. Welters and J. W. Weekamp, *Science*, 2001, **291**, 277–280.
8 B. S. Gallardo, V. K. Gupta, F. D. Eagerton, L. I. Jong, V. S. Craig, R. R. Shah and N. L. Abbott, *Science*, 1999, **283**, 57.
9 D. E. Kataoka and S. M. Troian, *Nature*, 1999, **402**, 794.
10 T. R. Kline, W. F. Paxton, Y. Wang, D. Velegol, T. E. Mallouk and A. Sen, *J. Am. Chem. Soc.*, 2005, **127**, 17150; T. R. Kline, J. Iwata, P. E. Lammert, E. E. Mallouk, A. Sen and D. Velegol, *J. Phys. Chem. B*, 2006, **110**, 24513; S. Subramanian and J. M. Catchmark, *J. Phys. Chem. C*, 2007, **111**, 11959; M. E. Ibele, Y. Wang, T. R. Kline, T. E. Mallouk and A. Sen, *J. Am. Chem. Soc.*, 2007, **129**, 7762.
11 W. F. Paxton, P. T. Baker, T. R. Kline, Y. Wang, T. E. Mallouk and A. Sen, *J. Am. Chem. Soc.*, 2008, **128**, 14881.
12 O. G. Schmidt and K. Eberl, *Nature*, 2001, **410**, 168.
13 Y. F. Mei, G. S. Huang, A. A. Solovev, E. Bermudez Urena, I. Mönch, F. Ding, T. Reindl, R. K. F. Fu, P. K. Chu and O. G. Schmidt, *Adv. Mater.*, 2008, **20**, 4085.
14 A. A. Solovev, Y. F. Mei, E. Bermudez Urena, G. S. Huang and O. G. Schmidt, *Small*, 2009, **5**(14), 1688.
15 A. A. Solovev, S. Sanchez, M. Pumera, Y. F. Mei and O. G. Schmidt, *Adv. Funct. Mater.*, 2010, **20**(15), 2430.
16 S. Sanchez, A. A. Solovev, Y. F. Mei and O. G. Schmidt, *J. Am. Chem. Soc.*, 2010, **132**, 13144.
17 S. Sanchez, A. A. Solovev, S. M. Harazim and O. G. Schmidt, *J. Am. Chem. Soc.*, 2010, **133**, 701.
18 S. Sanchez, A. A. Solovev, S. Schulze and O. G. Schmidt, *Chem. Commun.*, 2011, **47**, 698.
19 Y. F. Mei, A. A. Solovev, S. Sanchez and O. G. Schmidt, *Chem. Soc. Rev.*, 2011, DOI: 10.1039/c0cs00078g.
20 Y. H. Choi, S. U. Son and S. S. Lee, *Sens. Actuators, A*, 2004, **111**, 8; A. Takashima, K. Kojima and H. Suziki, *Anal. Chem.*, 2010, **82**, 6870–6876.
21 D. J. Thurmer, C. Deneke, Y. F. Mei and O. G. Schmidt, *Appl. Phys. Lett.*, 2006, **89**, 223507.
22 P. Tabeling, *Introduction to Microfluidics*, Oxford University Press, 2005.
23 S. K. Chung, Y. Zhao and S. K. Cho, *J. Micromech. Microeng.*, 2008, **18**, 095009.
24 G. A. Ozin, I. Manners, S. Fournier-Bidoz and A. Arsenault, *Adv. Mater.*, 2005, **17**(24), 3011.
25 I.-K. Jun and H. Hess, *Adv. Mater.*, 2010, **22**(43), 4823.
26 S. F. Jones, G. M. Evans and K. P. Galvin, *Adv. Colloid Interface Sci.*, 1999, **80**(1), 27.
27 E. J. Smith, S. Schulze, S. Kiravittaya, Y. F. Mei, S. Sanchez and O. G. Schmidt, *Nano Lett.*, 2011, DOI: 10.1021/nl1036148.